Corrosion Performance of the Shot-Peened High Strength Cu-alloy CuNi3SiMg in 0.1M NaCl

M. Gholami[1], F. Pastorek[2], M. Mhaede[1], M. Wollmann[1], B. Hadzima[2], I. Altenberger[3] and L. Wagner[1]

[1]Institute for Materials Science and Engineering, Clausthal University of Technology, Germany
[2]Research centre of the University of Žilina, Slovak republic
[3]Wieland - Werke AG, Central Laboratory, Ulm, Germany

Abstract
The present work was aimed at evaluating the effects of shot peening on corrosion performance of CuNi3SiMg alloy in 0.1M NaCl solution. A combination of rotary swaging and optimized precipitation hardening was applied to generate ultra-fine grained (UFG) microstructure. Shot peening to full coverage (100%) was performed using spherically conditioned cut wire (SCCW 14) with an average shot size of 0.36 mm at Almen intensities of 0.1, 0.17 and 0.25 mmA for solutionized, UFG and precipitation hardening conditions, respectively. After applying this mechanical treatment, the change in the surface and near surface layers was determined by surface roughness and microhardness measurements. Experimental investigations showed that an optimized combination of mechanical surface treatment and precipitation hardening condition reduces the corrosion rate in 0.1M NaCl solution by generating more favorable thermodynamic conditions for more proper formation of passive oxide layer with higher corrosion resistance.

Keywords CuNi3SiMg alloy, corrosion, 0.1M NaCl, shot peening.

Introduction

Copper and copper alloys often have excellent corrosion resistance, superior electrical and thermal conductivity as well as mechanical properties; therefore, they are widely used in industrial applications [1, 2]. However, Copper and its alloys can be very sensitive to aggressive corrosion ions like chloride, due to formation of an unstable film and soluble chloride complex as ($CuCl_2^-$) and $CuCl_3^{-2}$ [3]. The dissolution mechanism of Cu in NaCl is based on dissolution-precipitation [1, 2, 4, 5], results in the formation of diffusive compound $CuCl_2^-$ and precipitate CuCl on the surface as the concentration of $CuCl_2^-$ reached saturated limit [1, 2]. In most cases, failures like fatigue fracture, fretting fatigue, wear and corrosion occur on material surfaces. These failures are very sensitive to the structure and properties of the surface [6]. Mechanical surface treatment like shot peening will be able to enhance mechanical properties and corrosion resistance to aggressive environment [7]. The aim of this study is the evaluation of thermal and mechanical surface treatment on corrosion performance of CuNi3SiMg alloy in 0.1M NaCl solution.

Experimental Method

The investigated copper alloy is the Corson-type alloy CuNi3Si1Mg. It was delivered as rods of 23 mm diameter. The material condition in our present study was extruded, homogenized, and rotary swaged and subsequently precipitation hardened. Typical solution heat treatment (SHT) is 800°C for 2h. During swaging of solutionized samples at room temperature, the specimen diameters were reduced from 23 to 7 mm which correspond to a true deformation degree of 2.4 ($\varphi = 2.4$). Microstructure investigations were carried out on an optical microscope (Model: Zeiss Axioskop). The electrochemical measurements were carried out using a potentiostat/galvanostat/frequency response analyzer VSP from Biologic SAS France. At room temperature, 0.1 M NaCl solution was used as corrosive environment. Tafel polarization curves were obtained by changing the electrode

potential automatically from -200 mV_{SCE} to +200 mV_{SCE} at room temperature at open circuit potential with scan rate of $1mVs^{-1}$. Electrochemical impedance spectroscopy (EIS) measurements were performed at open circuit potential with AC voltage amplitude of 5 mV in a frequency range from 100 KHz to 1mHz. EIS measurements resulted in Nyquist plots that were further analyzed by software EC-Lab. Shot peening was performed with a direct pressure blast system using spherical conditioned cut wire (SCCW 14, 0.36 mm average shot size). The Almen intensities of 0.1, 0.17 and 0.25 mmA were used for SHT, SHT+SW (2.4) and SHT+SW (2.4) + age hardening conditions, respectively. The microhardness-depth-profiles were measured using a Struers Duramin Härteprüfer with a Vickers hardness pyramidal diamond indenter and an applied load of 100 gm.

Experimental Results

Fig.1 presents the microstructures comparing as-received (Ar) condition with conditions after solution treatment, severe plastic deformation and finally age hardening. The original samples were extruded at 900 °C, then solutionized at 800 °C/2h and subsequently water-quenched. The microstructure after this treatment exhibits a recrystallized coarse grain structure with twins within the grains. The precipitates responsible for the strengthening in the Cu-Ni-Si alloys have been identified as Ni_2Si [8, 9]. Coarse Ni-Silicides (diameter >200nm) were not dissolved at this homogenization temperature. Severe plastic deformation to a deformation degree of $\varphi = 2.4$, results in grain size refinement. In a swaged condition, the microstructures reveal no difference before and after age-hardening. The hardening particles are not visible in the optical microscope.

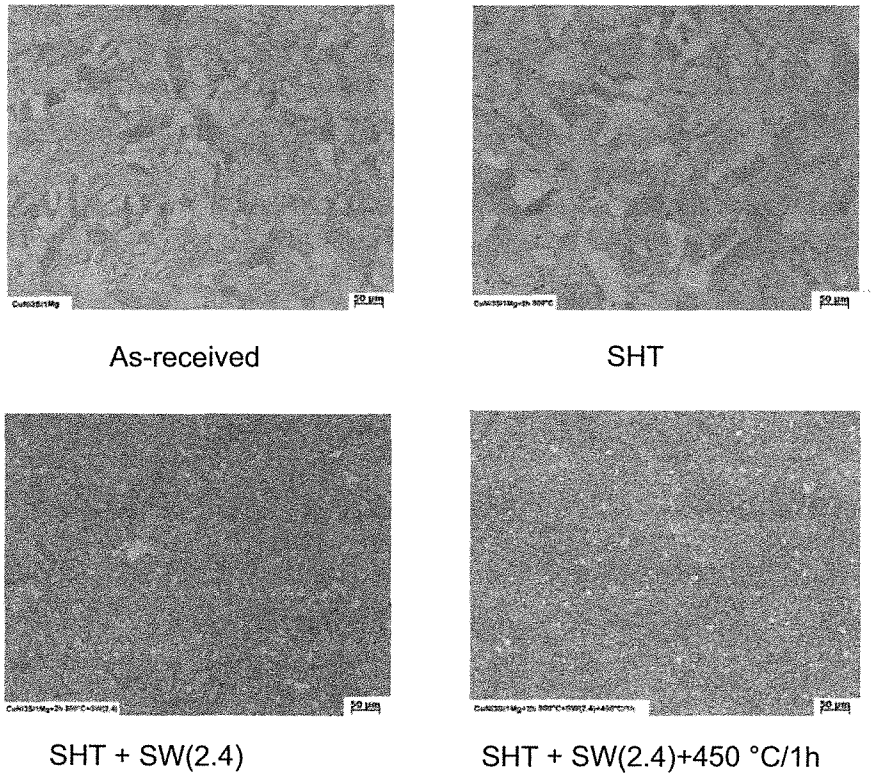

Fig. 1: Optical microstructure of CuNi3SiMg after SHT, SHT+SW (2.4) and age-hardening

The mechanical properties of CuNi3SiMg alloy in the initial, solutionized and after swaging and age-hardening were characterized in table 1. An analysis of the results showed that after solution

heat treatment, the material is very ductile. As expected, severe plastic deformation, SPD, led to an increase in tensile strength and yield stress. The work hardening capability which can be roughly estimated by (UTS-YS) is lowest in the condition SHT+SW (2.4) +450 °C/1h, 1MPa, in comparison with other conditions. It can be seen that aging for 1h at 450 °C results in an increase in both strength and elongation. The precipitates in CuNi3SiMg alloy with smaller grain size become finer due to the higher dislocation density. The dislocations as well as grain boundaries act as diffusion paths for solute atoms and provide nucleation sites for precipitation during aging treatment. The refinement of grain size and precipitate size were effective to enhance the tensile strength and elongation by reducing the inner-precipitate spacing [10].

Table1: Mechanical properties

Condition	YS (MPa)	UTS (MPa)	(UTS-YS) (MPa)	e_u (%)	El (%)	ε_F	HV 30
As-received	267	483	216	25	34	1.2	117
SHT	153	331	178	36	47	1.9	56
SHT+SW	587	588	1	0.2	0.5	1.5	161
SHT+SW+450°C/1h	821	845	24	6.5	11.6	0.5	230

Shot peening induces compressive residual stresses, work hardening and grain refinement in the surface layers. The formation of a passive film becomes complex when the surface has been altered by shot peening in comparison to a polished surface [11]. Table 2, indicates the surface roughness results on the shot peened samples in SHT, SHT+SW (2.4) and SHT+SW (2.4) +450 °C/1h conditions.

Table 2: Roughness Results

Condition	Roughness, Ra
SHT	1.76
SHT+SW	1.90
SHT+SW+450°C/1h	2.74

The microhardness values versus distance from the surface of specimens are presented in Fig. 2.

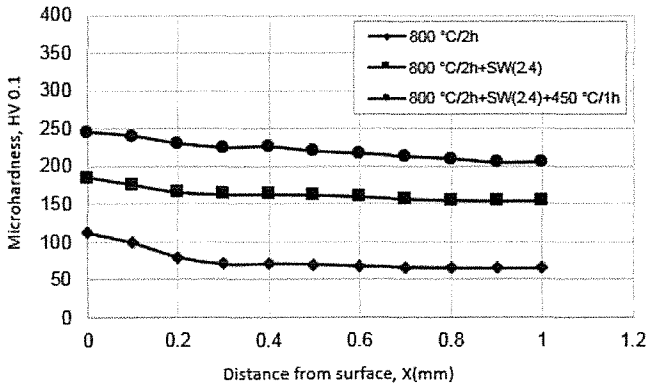

Fig. 2: Micro-hardness depth profiles

According to this figure, the hardness of SHT+SW (2.4) + aging is higher than shot peened specimens in conditions SHT+ SW (2.4) and SHT, respectively. Hardness decreases with a moderate slope until the depth of 1 mm. The hardness increase in specimen surface and its gradual decrease indicates the presence of compressive residual stresses and work hardening which is of

course decreased and disappeared with distancing from the surface [11]. Fig. 3, presents the potentiodynamic polarization curves before and after shot peening. The corrosion current density, i_{corr}, corrosion potential, E_{corr}, and corrosion rate values, C.R, estimated from the plots for each sample, are shown in table 3. The results indicate the slight differences in corrosion behaviors of SHT, SHT+SW (2.4) and SHT+SW (2.4) +450 °C /1h. After shot peening, SHT+SW (2.4) + 450 °C/1h and SHT+SW (2.4) conditions indicate better corrosion behavior as compared to SHT condition.

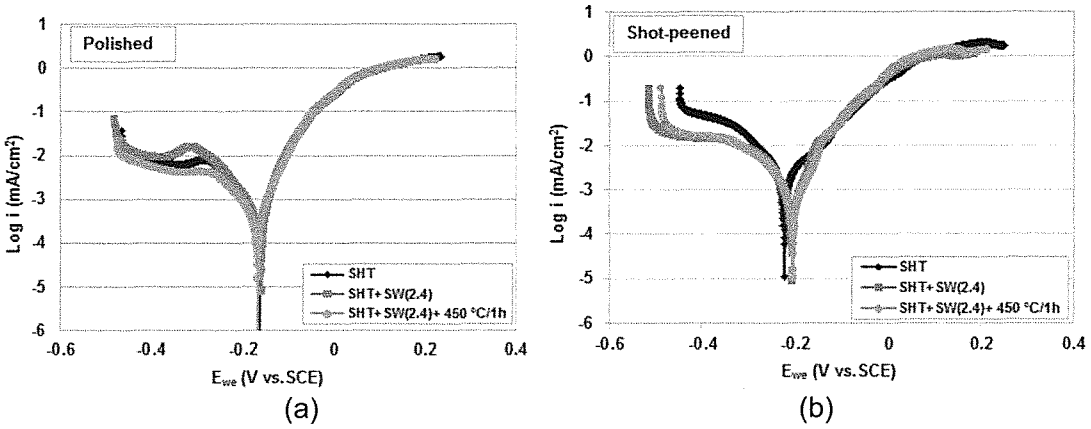

Fig. 3: Polarization curves of SHT, SHT+SW (2.4) and SHT+SW (2.4) +450 °C/1h (a) before and (b) after shot peening

Table 3: Potentiodynamic polarization parameters for the corrosion of CuNi3SiMg by 0.1 M NaCl

Condition	Surface Condition					
	Polished			Shot peened		
	icorr ($\mu A/cm^{-2}$)	Ecorr (mV)	C.R (mmpy)	iCorr ($\mu A/cm^{-2}$)	Ecorr (mV)	C.R (mmpy)
SHT	0.51	-161.9	1,143	2.38	-207.6	2.59
SHT+SW	0.49	-157.7	1.115	0.413	-206.4	0.97
SHT+SW+450 °C/1h	0.42	-166.6	1.016	0.3	-204.1	0.68

Fig. 4 shows the Nyquist plots of the impedance spectra for CuNi3SiMg alloy in 0.1 M NaCl before and after shot peening. It is interesting to note that the diameter of semicircular regions increases after SPD and SPD+ aging. The results were modelled using an equivalent circuit typical for coated surfaces, where $(CPE)_{dl}$, represents the capacity of the double layer, R_{ct}, the charge transfer resistance of the reaction taking place at the metal/solution interface, $(CPE)_{film}$, the capacity of a perfect film simulated as a non-idea capacitor (or constant phase element), and R_{film}, the resistance of the defects in the coatings. R_s, is the electrolyte resistance, Fig. 5 [12]. The corresponding impedance parameters are given in table 4.

The coating performance can be described by the coating capacitance and the resistance of the pore or defect in the coating. With an increase in the permeability of a coating, the conductive paths will be increased and this will lead to the reduction in the R_{ct}. It was noticed that there is an increase in R_{ct} and R_{film} in conditions SW (2.4) and SW (2.4) +450 °C/1h before and after shot peening.

Table 4: Parameters used in fitting of impedance data for CuNi3SiMg alloy in 0.1 M NaCl (a) before shot peening (b) after shot peening

CONDITION	R_s ($\Omega.cm^2$)	R_{film} ($\Omega.cm^2$)	$(CPE)_{film}$ ($e^{-3}F.s^{(a1)}$)	R_{ct} ($\Omega.cm^2$)	$(CPE)_{dl}$ ($e^{-3}F.s^{(a-1)}$)	R_p ($\Omega.cm^2$)
SHT	120	4217	5.4	7513	8.8	11730
SHT+SW	105	1746	3.2	16756	19.7	18502
SHT+SW+450 °C/1h	131	5960	2.4	17162	12.9	23122

(a)

CONDITION	R_s ($\Omega.cm^2$)	R_{film} ($\Omega.cm^2$)	$(CPE)_{film}$ ($e^{-3}F.s^{(a-1)}$)	R_{ct} ($\Omega.cm^2$)	$(CPE)_{dl}$ ($e^{-3}F.s^{(a-1)}$)	R_p ($\Omega.cm^2$)
SHT	100	1796	0.54	6831	8.8	8627
Sht+SW	131	6721	0.14	23522	2.5	30243
SHT+SW+450 °C/1h	100	7489	94.3	23378	3.6	30867

(b)

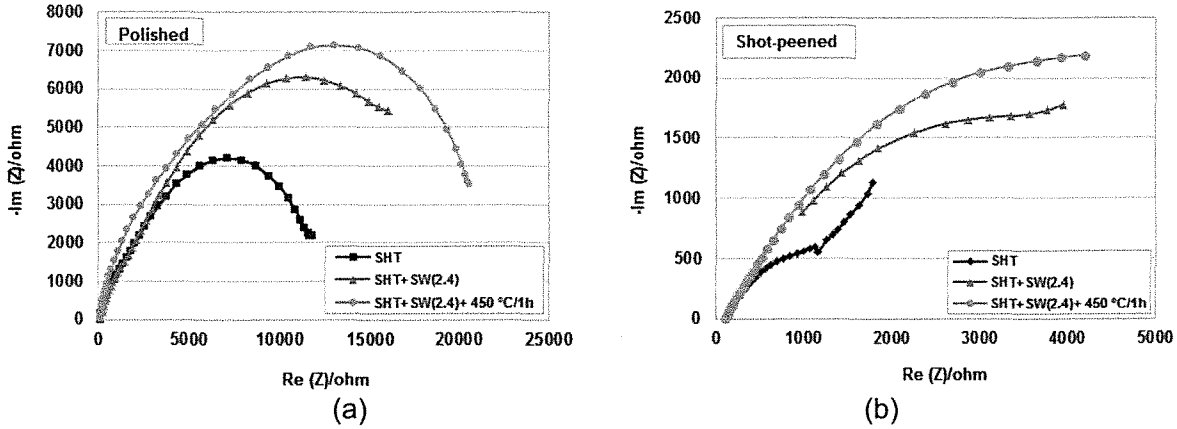

(a) (b)

Fig. 4: Nyquist plots of CuNi3SiMg alloy in 0.1 M NaCl (a) before shot peening (b) after shot peening

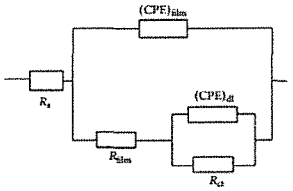

Fig. 5: Equivalent circuit used to calculate the Impedance parameters

Conclusion

SPD furnishes the CuNi3SiMg alloy with a uniform passive layer which results from the fine distribution of grain boundaries, acting as diffusion paths for elements migration [13,14,15]. The improvement of corrosion resistance of CuNi3SiMg alloy after age-hardening indicates the effect of precipitates and their uniform distribution on corrosion behavior [15]. Because of the inverse relationship between the corrosion resistance and surface roughness, corrosion behavior is likely not to be influenced by increasing roughness after shot peening. The hardness increase in specimens' surface after shot peening shows the presence of compressive residual stresses, work hardening and high density of grain boundaries which enhance the formation of passive film at the samples' surface that consequently improves corrosion resistance through restriction of interaction between metal ions and corrosion environment [11]. In this study, the effect of fine grains,

compressive residual stress and work hardening at the samples' surfaces in SHT+SW (2.4) + aging and SHT+SW (2.4) conditions after shot peening, seem to be more dominant than roughness [16].

Acknowledgment

The research is supported by European Regional Development Fund and Slovak state budget by the project "Research Centre of the University of Žilina", ITMS 26220220183.

References

[1] J.Crousier, A.-M.Beccaria, *Behavior of Cu-Ni alloys in natural sea water and NaCl solution,* Werkstoffe und Korrosion, Vol.41 (1990), pp 185-189.

[2] M.M.Al.Abdollah, A.K.Maayta, M.A.Al-Qudah, N.A.F.Al-Rawashdeh, *Corrosion Behavior of Copper in Chloride Media*, the Open Corrosion Journal, Vol.2 (2009), pp 71-76.

[3] C.W:Yeow ,D.B.Hibber,*Galvanostatic Pulse Plating of Copper and Copper (I) Halides from Acid Copper (II) Halide Solution* ,J.Electrochem Soc.,Vol.130 (1983) , pp 786-790.

[4] K.F.Khaled, *Studies of the Corrosion Inhibition of copper in Sodium Chloride Solution Using Chemical and Electrochemical Measurements*, Materials Chemistry and Physics, Vol.125 (2011), pp 427-433.

[5] J.Crousier, L.Pardessus, J.P.Crousier, *Voltammetry Study of Copper in Chloride Solution*, Electrochim Acta, Vol.33 (1988), pp 1039-1042.

[6] K.Lu, J.Lu, *Nanostructured surface layer on metallic materials induced by surface Mechanical attrition treatment*, Material Sci.and Eng. A, 375-377 (2004), 38-45.

[7] T.Wang, I.Yu, Bingfeng Dong, *Surface Nanocrystallization Induced by Shot peening and Its Effect on Corrosion Resistance of 1Cr18Ni9Ti Stainless Steel*, Surface&Coatings Tec. Vol.200 (2006) 4777-4781.

[8] R.Monzen, C.Watanabe, *Microstructure and Mechanical Properties of Cu-Ni-Si alloys*, Material Science and Engineering A, 483-484 (2008), pp 117-119.

[9] S.A.Lockyer, F.W.Noble, *Precipitate Structure in Cu-Ni-Si alloy*, J.Mater.Scie, Vol.29 (1994), pp 218-226.

[10] HO J.RYU, HYUNG K.BAIK, SOON H.HONG, *Effect of Thermomechanical treatments on Microstructure and Properties of Cu-based Leadframe alloy*, J.Mater.Scie, Vol.35 (2000), pp 3641-3646.

[11] V.Azar,B.Hashemi, Mahboobeh Rezaee Yazdi , *The Effect of Shot peening on Fatigue and Corrosion Behavior of 316L Stainless Steel in Ringer's Solution*, Surface &Coation Tech.,Vol.204 (2010) ,pp 3546-3551.

[12] Venkata APPa ,Rao Boyapati, Chaitanya Kumar Kanukula,*Corrosion Inhibition of Cu-Ni (90/10) Alloy in Seawater and Sulphide-Polluted Seawater Environments by 1,2,3-Benzotriazole*,ISRN Corrosion,Vol.2013,22 pages.

[13] Song Dan,MA Ai-bin,JIANG Jing-hua,LIN Pin-hua,YANG Dong-hui,*Corrosion behavior of ultra-fine grained industrial pure Al fabricated by ECAP*,Trans.Nonferrous Met.Soc.China, Vol.19(2009) , pp 1065-1070.

[14] X.Y.Wang,D.Y.Li,*Mechanical and Electrochemical behavior of nanocrystalline surface of 304 Stainless Steel*, Electrochim Acta,Vol.47(2002) pp 3939-3947.

[15] Jeong-Yong Park,Yong-Hwan Jeong and Youn-Ho Jung,*Effects of precipitation Characteristics on the out –Pile Corrosion Behavior of Niobium-Containing Zirconium Alloys*,Metals and Materials international,Vol.7,No.5 (2001),pp 447-455.

[16] Suyitno, M. Mahardika, P. Dewo, B. Arifvianto, Study on surface properties and corrosion resistance of 316L stainless steel processed with steel slag ball blasting treatment, 9th International Conference ON Fracture & Strength of Solids, June 9-13, 2013, Jeju, Korea.